Photochemically Induced Reactions of Ozone with 1,2-Dibromoethene and 1,2-Dichloroethene: An FT-IR Matrix Isolation Study†

Robin J. H. Clark* and Loraine J. Foley

Christopher Ingold Laboratories, University College London, 20 Gordon Street, London WC1H 0AJ, UK

Received: May 4, 2001

The co-deposition of ozone with the halogenated ethenes, 1,2-dibromoethene and 1,2-dichloroethene, in argon matrices and the subsequent photolysis cycles using radiation of different wavelengths ($\lambda > 350$ nm, $\lambda > 290$ nm, and $\lambda > 240$ nm) have been examined using FT-IR spectroscopy. Ozonolysis occurs after irradiation at relatively long wavelengths, ($\lambda > 350$ nm), due to the formation of an ozone···XCH═CHX (X = Br or Cl) π complex upon deposition and is believed to follow the Criegee pathway because the expected HC(O)X (X = Br or Cl) intermediates are detected. The carbonyl species HC(O)X dissociate to form the carbon monoxide species, OC···HX and OC···$(HX)_2$ (X = Br or Cl). However, the identification of a novel ketene species XHC═C═O suggests that a further mechanism to the Criegee one is followed in the case of halogenated ethenes. Moreover the photochemically induced reaction of XCH═CHX deposited in oxygen matrices produced the similar photoproducts HC(O)X and OC···HX as well as the ketene type species XHC═C═O, providing additional evidence that a further mechanism is being followed from that involved in ozonolysis. Two possible reaction pathways involving either the ozone molecule or oxygen atoms are discussed.

Introduction

The gas-phase reactions of ozone with alkenes have attracted considerable attention over the years,[1−10] especially in the last few, due to their possible relevance to atmospheric chemistry.[7,11−13] The mechanism of the ozonolysis of alkenes, first proposed by Criegee in 1951,[14] has received substantial experimental support and is now accepted. The reaction leads to the oxidative cleavage of the double bond and the formation of aldehydes and/or ketones or their peroxidic derivatives. The three-step mechanism involves three intermediates, the primary ozonide (1,2,3-trioxolane, POZ), a carbonyl oxide (Criegee intermediate, CI) and carbonyl compound, and the secondary ozonide (1,2,4-trioxolane, SOZ).[14] The Criegee intermediate can degrade by different decomposition and isomerization pathways in the gas phase leading to a variety of oxygenated organic products. Later work revealed the presence of an ozone···alkene charge-transfer complex[9,15−18] which is presumably the precursor of the POZ.

Matrix isolation studies of the ozone/alkene reaction have made possible the full characterization of the POZ and SOZ intermediates by infrared spectroscopy.[2,3,6,9] However to initiate the reaction, most of the matrices had to be warmed to relatively high temperatures (77 K for a N_2 matrix,[3] 80−100 K for a Xe matrix,[6] 25 K for an amorphous CO_2 matrix,[9] 77 K for a crystalline CO_2 matrix,[9] and 44 K for an Ar matrix[9]) before any new bands appeared. Besides ozonolysis, the oxidation of halogenated alkenes with $O(^3P)$ atoms[19,20] or O_2[21,22] has been shown to afford a range of oxygenated organic products and to eliminate small molecules such as CO, CO_2, and X_2. Furthermore, in some studies the elimination of HCl has been noted from chlorinated alkenes upon photolysis to yield an alkyne species. [23−25]

The aim of this work is to analyze the photochemically induced reactions of 1,2-dibromoethene and 1,2-dichloroethene with ozone in argon matrices; this is an extension of the simple alkene/ozone reactions studied previously in the gas phase as well as an extension of the halogenated alkane/ozone reactions studied previously by matrix techniques.[26,27] It is of interest to establish whether irradiation, instead of annealing, can initiate ozonolysis in an argon matrix via the Criegee mechanism and whether the halogen substituents have any effect on the reaction mechanism. Oxygen atom oxidation may occur instead of ozonolysis resulting in the decomposition of the halogenoethene. The question of whether an ozone···CHXCHX (X = Br or Cl) charge-transfer complex will form is also of interest.

Experimental Section

Ozone was generated by Tesla coil discharge through either normal oxygen, oxygen-18 or a 1:1 mixture of each contained in a 10 cm Pyrex finger immersed in liquid nitrogen. Ozone was obtained in a blue condensed form and purified by multiple freeze−thaw cycles to remove any residual oxygen. British Oxygen Co. supplied the research grade oxygen (>99.9%) and argon, whereas oxygen-18 (>97.7%) was supplied by Enritech Enrichment Technologies Ltd. 1,2-dibromoethene and 1,2-dichloroethene were both purchased from Aldrich and used as supplied.

In a typical experiment, the halogenated ethenes were diluted separately at species-to-argon (S/Ar) ratios in the range from 1:1000 to 1:3000 by use of standard manometric procedures at room temperature. The precursor gas mixtures were then deposited for 6 h at rates of approximately 3 mmol h^{-1} onto a cold (14 K) CsI window mounted in a Displex closed-cycle helium cryostat (Air Products DE 202 S). The vacuum shroud surrounding the cold window could be aligned for infrared transmission studies, for gas deposition, or for sample photolysis. Infrared spectra were recorded on a Bruker IFS 113v FT-IR

† Part of the special issue "Mitsuo Tasumi Festschrift".

* To whom correspondence should be addressed. E-mail: rjhclark@ucl.ac.uk. Fax: +44 (0) 20 7679 7463.

10.1021/jp011707q CCC: $22.00
Published on Web 09/06/2001

spectrometer over the range 500−4000 cm^{-1} at a resolution of 0.5 cm^{-1} using a germanium-coated KBr beam splitter and a MCT detector cooled with liquid nitrogen. The band wavenumbers observed are accurate to ±0.2 cm^{-1} for sharp bands. A DTGS detector was used to record spectra over the range 600−200 cm^{-1} at a resolution of 1 cm^{-1}. Spectra were recorded after each matrix irradiation or warming cycle to monitor any changes caused by these processes. The matrices were irradiated for various periods of time with an Oriel xenon mercury lamp, a 5 cm thick water filter being placed between the lamp and the sample to reduce the infrared output of the lamp. Filtered radiation in the visible and ultraviolet regions was selected by use of the following transmission filters: Corning 7 mm thick blue/green ($550 > \lambda > 350$ nm), Pyrex ($\lambda > 290$ nm), and quartz ($\lambda > 240$ nm). In this way, the wavelength selectivity of the product distribution could be established.

Results and Discussion

Precursor Deposition in Argon and in Oxygen Matrices. The infrared spectra of *cis*- and *trans*-1,2-dibromoethene, BrCH═CHBr, isolated in an argon matrix (BrCH═CHBr/Ar = 1:3000) and in an oxygen matrix (BrCH═CHBr/O_2 = 1:2500) were recorded (Table 1), as were the infrared spectra of *trans*-1,2-dichloroethene, ClCH═CHCl, isolated in an argon matrix (ClCH═CHCl/Ar = 1:1000) and in an oxygen matrix (ClCH═CHCl/O_2 = 1:1000) (Table 2). The band wavenumbers in both cases were assigned using as guides the assignments of bands for ethene[28−30] and other halogenoethenes[23−25] in matrices. Ultraviolet photolysis ($\lambda > 240$ nm) of BrCH═CHBr (*cis* or *trans*) or ClCH═CHCl (*trans*) deposited in an argon matrix produced no new bands. By contrast, it should be noted that when dichloroethenes are photolyzed ($\lambda > \sim 240$ nm) in krypton or xenon matrices they undergo elimination of Cl_2 or HCl to produce an alkyne complex, $C_2H_2\cdots Cl_2$ or $C_2HCl\cdots HCl$.[24,25]

Co-deposition with Ozone. The infrared spectrum of either BrCH═CHBr or ClCH═CHCl co-deposited with ozone in an argon matrix (BrCH═CHBr/O_3/Ar = 1:3:2000; ClCH═CHCl/O_3/Ar = 1:2.5:2500) exhibited bands that resembled those detected in the infrared spectra of BrCH═CHBr, ClCH═CHCl, or ozone[31−33] isolated separately in argon (Tables 1 and 2). In addition, however, weak bands with small wavenumber shifts from the fundamental bands of ozone were detected in these experiments on BrCH═CHBr/O_3 and ClCH═CHCl/O_3 and are attributed to an ozone···precursor complex. This initial interaction between ozone and the halogenoethene occurs at the double bond of the alkene (an electron-donating area) thereby forming a charge-transfer complex. The appearance of $\nu_{C=C}$ bands slightly shifted from those detected for isolated BrCH═CHBr or ClCH═CHCl provides further evidence that such a complex is present. The bands attributed to either the ozone···BrCH═CHBr charge-transfer complex or the ozone···ClCH═CHCl charge-transfer complex began to deplete upon UV−vis irradiation ($\lambda > 350$ nm), whereas those belonging to further new species began to grow in. The formation and characterization of ozone complexes with other carbon π systems have been explored elsewhere.[8,9,15−18]

Varying the deposition ratios of BrCH═CHBr/O_3/Ar or ClCH═CHCl/O_3/Ar made no difference to the photochemistry but caused the intensities of the precursor bands to increase or decrease according to whether the concentrations were increased or decreased. Also, an increase in the intensities of the precursor bands resulted in an increase in the intensities of the bands attributable to the complexes. In addition to the precursor bands, small quantities of matrix-isolated water and carbon dioxide were detected. Isotopic ozone, $^{18}O_3$, and mixed-ozone, $^{16}O_{3-x}{}^{18}O_x$, samples have also been condensed with either 1,2-dibromoethene or 1,2-dichloroethene in argon matrices (Tables 1 and 2). In each case, the sextet of bands for each vibrational mode of the six isotopomers of ozone was detected and their wavenumbers agreed with those reported elsewhere for isolated ozone.[31−33] Bands for complexed ozone could also be detected alongside those for isolated ozone.

TABLE 1: Infrared Bands (cm^{-1}) Recorded after Deposition of *cis*- and *trans*-BrCH═CHBr in Different Matrices at 14 K

Ar	O_2[a]	$^{16}O_3$/Ar	$^{18}O_3$/Ar	assignment
3107.9w	3100.8w		3107.6mw	$\nu_{a\ C-H}$
	3089.1w[b]			
3076.1vw, sh	3077.9w	3074ms, br	3075.9w	$\beta_{s\ C-H}$
3073.7w[b]	3072.0w[b]		3073.6mw[b]	
		2140.7vw	2140.7vw	(CO···H_2O) **?**
		2110.8w[b]	1996.5vw[b]	$3\nu_2$ (O_3)
		2108.3w	1993.6mw	
		2103.7w[c]		
1592.7w[b]			1593.1w[b]	$\nu_{C=C}$[d]
1590.3mw	1589.8m	1589.6s, sh	1590.2mw	
		1588.1s[c]	1588.4w, sh[c]	
	1549.7w	1541.4mw	1541.8w	?
1536.9w	1548.3 w	1536.9mw	1536.8w	?
1494.5vw	1497.2vw	1494.3w	1494.4vw	$2\nu_{a\ C-Br}$
		1493.1w[b]	1492.8vw[b]	
1261.1w[b]			1261.1w[b]	δ_{CHBr} (i−p)[d]
1259.4mw	1259.9mw		1259.4m	
1258.9w,sh[b]		1255ms, br[b]		
1162.2mw	1164.4mw	1161.9s	1162.0m	δ_{CHBr} (i−p)[e]
1161.4w,sh		1159.1s		
1151.0vw	1151.3vw	1149.2mw	1151.0w	
		1040.5ms[b]	984.6ms, sh[b]	ν_3 (O_3)
		1039.3s	983.4s	
		1037.9ms[b]	982.3s[b]	
		1033.5ms[c]	980.8ms[b]	
		1031.8m, sh[c]	978.9mw[c]	
			976.9mw[c]	
914.5vw			914.2mw	δ_{CHBr} (o−o−p)[e]
912.4mw		912.0m	912.2m	
908.5w	906.1m		908.4w	
900.2vw	904.3mw, sh	901s, br		
898.9vw, sh				
897.3vw				
753.2m	754.8ms		753.1ms	$\nu_{a\ C-Br}$
752.2mw, sh		752.4vs	752.3ms	
		751.5vs		
		750.8vs, sh		
		703.0w, br	665.2w	ν_2 (O_3)
694.5mw	689.5m	694.0mw	694.3m	δ_{CHBr} (o−o−p)[d]
690.2vw	685.2m	685.9vs		
		684.5vs		
		683.4vs		
	679.1mw, sh	681.6vs		
675.1mw	676.5mw	675.2s	675.1m	
673.4w			673.4mw	
672.0mw		672.2s	672.0mw	
587.8w	588.3w	585.1m	587.5w	γ_{CHBr}[d]

[a] Bands slightly shifted in the O_2 matrix. [b] Bands due to matrix site effects. [c] Bands of complex. [d] Bands attributed to *cis*-BrCH═CHBr only. [e] Bands attributed to *trans*-BrCH═CHBr only.

Behavior of the Deposited Precursors after Photolysis. Subsequent photolysis of argon matrices containing either BrCH═CHBr/O_3 or ClCH═CHCl/O_3 led to the formation of new bands which are grouped according to the chemical species to which they refer.

Carbonyl Species. Many new bands in the carbonyl stretching region were detected after UV−vis irradiation ($\lambda > 350$ nm) of BrCH═CHBr/O_3 and ClCH═CHCl/O_3 matrices and their intensities increased very slightly upon Pyrex- ($\lambda > 290$ nm) and quartz-filtered ($\lambda > 240$ nm) irradiation. The carbonyl bands

TABLE 2: Infrared Bands (cm^{-1}) Detected after Deposition of *trans*-ClCH═CHCl in Different Matrices at 14 K

Ar	O_2	$^{16}O_3$/Ar	$^{18}O_3$/Ar	assignment
3109.2m	3099.9ms	3109.8w	3109.6m	
3105.8mw, sh[a]	3090.6ms, sh[a]	3105.5vw, sh[a]	3105.4mw[a]	$\nu_{a\ C-H}$
3103.0w, sh[a]	3076.8mw[a]	3103.6vw, sh[a]		
3080.1w				$\nu_{s\ C-H}$
		2149.3w		$\nu_1 + \nu_3$ (O_3)
		2143.2vw[a]		
		2140.6vw		(CO···H_2O) **?**
		2137.9vw[a]		
		2111.0vw[a]	1996.0mw[a]	
		2108.4w	1993.6mw	$3\nu_2$ (O_3)
1601.9mw[a]		1602.0mw[a]	1601.9mw[a]	
1599.4mw	1595.8ms	1599.4mw	1599.5mw	
			1598.0mw[c]	
1597.1w[a]			1597.0mw[a]	$\nu_{C=C}$[b]
		1595.7w[c]		
1593.4w[a]		1593.4w[a]	1593.4mw[a]	
1589.4w[a]		1590.5w[a]		
1211.3vw[a]				
1203.3mw, sh[a]	1204.9s[a]	1203.3w, sh[a]	1202.9m, sh[a]	
1201.8ms[a]	1203.6s, sh[a]	1202.0mw	1201.9ms[a]	δ_{CHCl} (i−p)
1200.5m, sh	1201.3s, sh		1200.4mw, sh	
		1046.8mw[a]		
		1040.6ms[a]		
		1039.4s	980s, br	ν_3 (O3)
		1037.9m[a]	977.8s, sh[c]	
		1034.8mw, sh[c]		
		912.1w, sh		
909.7s		910.2mw	909.8s	
905.9ms	904vs, br	906.3w	906.0ms	
902.8m, sh			903.0m, sh	δ_{CHCl} (o−o−p)[a]
901.9m, sh	901.9vs, sh			
	900.1vs, sh			
851.2w	848.5mw			
827.3vs		827.4m	827.2vs	
824.4vs		824.4m	824.3vs	
821.5s		821.5mw	823.3vs	$\nu_{a\ C-Cl}$[d]
			821.6vs	
818.9ms, sh	818vs, br	818.6mw, sh		
		704.5vw		ν_2 (O_3)

[a] Bands due to aggregates or matrix site effects. [b] The $\nu_{C=C}$ stretch of *trans*-ClCH═CHCl is infrared inactive although it does give rise to a band in the spectrum due to lowered symmetry in the matrix. [c] Bands of complex. [d] Many bands may be due to isotopic splitting.

are the most diagnostic for identifying the different carbonyl···Lewis acid complexes present in a matrix.

HC(O)X (where X = Br or Cl). After UV−vis photolysis of a BrCH═CHBr/O_3 matrix, new bands occurred in the carbonyl region of the infrared spectrum and some of these are assigned to $\nu_{C=O}$ of formyl bromide in different environments (Table 3 and Figure 1). For example, the very weak and weak bands situated at 1804.5 and 1801.1 cm^{-1} are indicative of HC(O)Br isolated in argon ($\nu_{C=O}$ = 1801.5 cm^{-1} [26] and 1799 cm^{-1} [34]), whereas those detected weakly between 1756.7 and 1747.9 cm^{-1} are indicative of HC(O)Br perturbed by the Lewis acid, HBr ($\nu_{C=O}$ = 1756.3 cm^{-1}).[27] Bands detected between 1734.6 and 1730.0 cm^{-1} are assigned to $\nu_{C=O}$ in an even more perturbing environment such as HC(O)Br···$(HBr)_2$. In the ^{18}O-enriched matrices, the $\nu_{C=O}$ band belonging to the formyl bromide isotopomer HC(^{18}O)Br was expected to occur at ∼1742 cm^{-1} (^{18}O-shift of ∼57 cm^{-1}),[27] whereas $\nu_{C=O}$ of HC(^{18}O)Br···HBr was expected to occur at ∼1715 cm^{-1}.[27] However, neither of these species could be detected in the BrCH═CHBr/$^{18}O_3$ experiment, although HC(O)Br and HC(O)Br···HBr could be, albeit weakly, in the BrCH═CHBr/$^{16}O_3$ experiment. A set of bands occurring at lower wavenumbers than expected for $\nu_{C=O}$ of HC(^{18}O)Br···HBr, appeared between 1709.6 and 1706.7 cm^{-1} and could possibly belong to HC(^{18}O)Br in an even more perturbing environment, i.e., HC(^{18}O)Br···$(HBr)_2$. Another band

TABLE 3: Infrared Bands (cm^{-1}) Assigned to $\nu_{C=O}$ and Detected after Quartz-Filtered (λ > 240 nm) Photolysis of Different Matrices Containing *cis*- and *trans*-BrCH═CHBr at 14 K[a]

$^{16}O_3$/Ar	$^{18}O_3$/Ar	$^{16}O_{3-x}{}^{18}O_x$/Ar	O_2	species
1831.8vvw				
1819.4vw, sh				
1814.2vw, sh				$CH_2BrC(O)Br$ **?**
1812.4vw				
1809.6vw, sh				
1804.5vw, sh				HC(^{16}O)Br
1801.1w, sh				
1797.0w				
1795.3w, sh				
1793.4w, sh				
1788.2w, sh				?
1785.3w				
1783.2w, sh				
1772.4w, sh				HC(^{16}O)Br···Br_2 **?**
1767.8w, sh				
1765.2w, sh				
1763.8w				$(HC(O)Br)_2$ **?**
1759.0w, sh				
1756.7w				
1755.5w, sh				
1753.5w				HC(^{16}O)Br···HBr[b]
1747.9w, sh				
1740.1mw		1740.0vw	1740.1vw	HC(^{16}O)H
1734.6mw, sh		1734.7vw	1734.2vw	
1733.4mw		1733.6vw, sh		HC(^{16}O)Br···$(HBr)_2$[b]
1730.0w, sh		1730.1vw		
1726.6w, sh		1723.3w, sh	1724.5vw	
1721.0w, sh		1722.0w	1721.1vw	
		1719.0vw	1719.6vw, sh	HC(^{16}O)H···HBr[b]
1716.0w, sh			1718.8vw	
		1717.6vw, sh		HC(^{18}O)Br···HBr[b]
		1709.6vw, sh		
		1708.0vw		HC(^{18}O)Br···$(HBr)_2$[b]
		1706.7vw		
	1704.1mw	1704.0w		
	1703.9mw, sh			HC(^{18}O)H
	1703.4mw, sh			
		1700.9w, sh		
	1698.7vw	1699.1mw		
	1696.2vw	1696.2w, sh		HC(^{18}O)H···HBr[b]
		1694.6w		
		1685.3vw		

[a] The large number of bands may be due to aggregates or to matrix site effects. [b] Lewis acid HBr of the nearest neighbor.

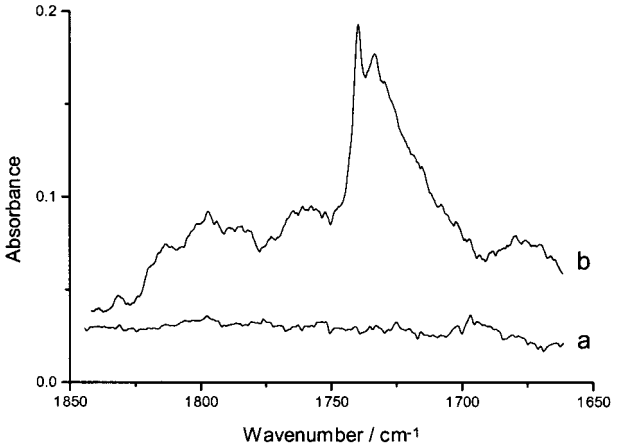

Figure 1. Infrared spectra of a BrCH═CHBr/$^{16}O_3$/Ar matrix after (a) deposition and (b) quartz-filtered photolysis (λ > 240 nm). The spectra show bands assigned to $\nu_{C=O}$ of new species.

attributed to formyl bromide was detected at 637.2 cm^{-1} (at 636.9 and 631.9 cm^{-1} in the $^{18}O_3$ experiment) and is assigned to ν_{C-Br}.

In the analogous ClCH═CHCl/O_3 experiment, new bands assigned to $\nu_{C=O}$ were detected after photolysis between 1761.8

TABLE 4: Infrared Bands (cm^{-1}) Assigned to $\nu_{C=O}$ and Detected after Quartz-Filtered ($\lambda > 240$ nm) Photolysis of Matrices Containing *trans*-ClCH=CHCl at 14 K[a]

$^{16}O_3$/Ar	$^{18}O_3$/Ar	$^{16}O_{3-x}{}^{18}O_x$/Ar	O_2	species
		1831.0w		$CH_2ClC(O)Cl$?
		1819.2w		
		1808.8w, sh		
		1805.0w, sh		
		1802.6w, sh	1803 mw,br	$ClC(O)Cl$[b] ?
		1799.8w, sh		?
		1796.2w, sh		?
		1792.9w		?
		1788.5w		?
		1787.3w		?
		1782.6mw, sh		$HC(^{16}O)Cl$
		1780.6mw		
		1775.0 mw		$(HC(O)Cl)_2$
		1772.9mw		
		1771.5mw, sh		
		1768.1mw	1768.3mw, br	
		1765.3mw, sh		
		1763.1mw, sh		
1761.8vw		1760.2mw, sh		$HC(^{16}O)Cl\cdots HCl$[c]
1756.5vw		1756.2mw, sh	1757.3m, sh	
1751.5w		1751.8m	1752.2m	
		1749.4mw, sh	1748.7m, sh	
		1747.2mw, sh		$HC(^{16}O)H$
1746.5w, sh		1745.3m	1745.2m, sh	
1744.7w				
1741.6vw, sh		1741.6mw, sh		
	1751.5mw, sh			$HC(^{18}O)Cl$
	1748.8mw			
	1747.1mw, sh	1747.2mw, sh		
	1746.0mw, sh	1745.3m		
	1743.7mw, sh			
	1741.1w	1741.6mw, sh		
	1739.9mw			
	1734.5w	1734.9mw, sh	1735.2mw, sh	?
1733.5vw	1733.5w	1733.6mw, sh		?
	1730.0w		1730.3mw, sh	?
	1723.5mw, sh	1723.6mw, sh		?
	1720.5mw	1720.6mw		?
		1719.6mw		$HC(^{16}O)H\cdots(HCl)_2$[c]
1718.4vw		1718.8mw, sh		
1717.2vw				
1715.8vw, sh				
	1715.1mw	1715.2mw		$HC(^{18}O)Cl\cdots HCl$[c]
	1714.3mw, sh			
	1712.8mw			
	1711.3mw, sh			
	1710.0mw, sh			
	1708.5mw	1708.6mw		$HC(^{18}O)H$
	1706.5mw	1706.8mw		
	1704.4m	1704.5mw		
	1700.9mw, sh			
	1700.0mw, sh	1699.3mw, sh		$HC(^{18}O)H\cdots HCl$[c]
	1697.9mw, sh	1698.1mw, sh		
	1696.0mw			

[a] The large number of bands may be due to aggregates or to matrix site effects. [b] $\nu_{C=O}$ of ClC(O)Cl = 1803 cm^{-1}.[37] [c] The HCl comes from the nearest neighbor.

and 1751.5 cm^{-1} (Table 4) and are attributed to formyl chloride HC(O)Cl perturbed by the Lewis acid HCl (Figure 2). Bands belonging to the unperturbed species were expected to occur around ~1780 cm^{-1} [26,35] but were too weak to be detected, although they could be detected in the mixed-ozone experiment. The shift in $\nu_{C=O}$ of HC(O)Cl···HCl from that of isolated HC(O)Cl compares well with those observed for other carbonyl···HCl complexes.[26,27] In the $^{18}O_3$ experiments, bands occurring between 1751.5 and 1739.9 cm^{-1} are assigned to $\nu_{C=O}$ of $HC(^{18}O)Cl$ isolated in argon, based on the ^{18}O-shift of ~40 cm^{-1} for the $HC(^{16/18}O)Cl\cdots HCl$ pair reported elsewhere.[27] The attribution of medium-weak bands, detected between 1715.1 and 1710.0 cm^{-1}, to $HC(^{18}O)Cl\cdots HCl$ is made on the basis that the ^{18}O-shift reported for the $HC(^{16/18}O)Cl\cdots HCl$ pair[27] is similar to that observed here. Both sets of isotopomer bands were detected in the mixed-ozone experiment indicating that only one ^{16}O or ^{18}O atom is present in the molecule (Figure 2).

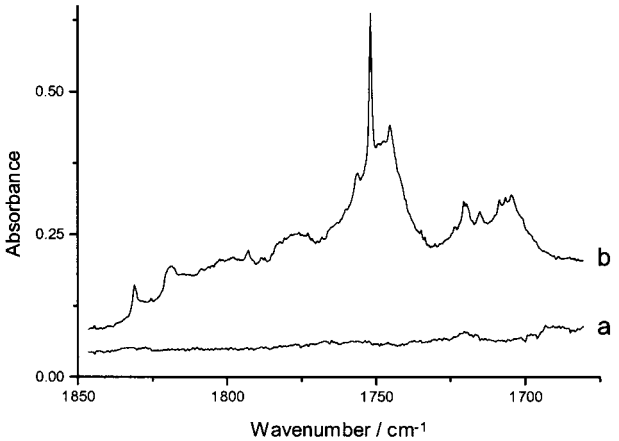

Figure 2. Infrared spectra of a ClCH=CHCl/$^{16}O_{3-x}{}^{18}O_x$/Ar matrix after (a) deposition and (b) quartz-filtered irradiation ($\lambda > 240$ nm), showing the appearance of new bands in the $\nu_{C=O}$ region.

HC(O)H. In the BrCH=CHBr/O_3 experiment, the band occurring in the carbonyl stretching region at 1740.1 cm^{-1} (Table 3) possibly belongs to isolated formaldehyde, HC(O)H, on the basis that its wavenumber agrees well with that detected for HC(O)H in the gas phase (1746.1 cm^{-1})[36] (1743.6 cm^{-1}),[37] in nitrogen matrices (1739.9 cm^{-1})[36] (1740.3 cm^{-1}),[38] and in argon matrices (1742.0 cm^{-1})[36] (1742.5 cm^{-1}).[27] A band attributed to $HC(^{18}O)H$ appeared in the ^{18}O-enriched ozone experiments at 1704.1 cm^{-1}, along with shoulders at 1703.9 and 1703.4 cm^{-1}. The ^{18}O-shift of 36.0 cm^{-1} is consistent with that observed for the $HC(^{16}O)H/HC(^{18}O)H$ pair studied elsewhere (34.2 cm^{-1}).[27] Other $\nu_{C=O}$ bands, red-shifted to 1726.6, 1721.0, and possibly 1716.0 cm^{-1}, are attributed to the carbonyl···Lewis acid complex HC(O)H···HBr ($\nu_{C=O}$ = 1727.9 cm^{-1} for HC(O)H···HBr in solid argon)[39] whereas the ^{18}O isotopomer bands occurred at 1698.7 and 1696.2 cm^{-1} (Table 3). Bands characteristic of formaldehyde, HC(O)H, were also detected after UV−vis irradiation of ClCH=CHCl/O_3 matrices (Table 4 and Figure 2). For instance, those occurring at 1746.5, 1744.7, and 1741.6 cm^{-1} are assigned to $\nu_{C=O}$ of HC(O)H, cf. $\nu_{C=O}$ = 1746.1 cm^{-1} (HC(O)H in the gas phase),[36] $\nu_{C=O}$ = 1742.0 cm^{-1} (HC(O)H in an argon matrix).[36] Bands belonging to the ^{18}O isotopic counterpart appeared at 1708.5, 1706.5, 1704.4, and 1700.9 cm^{-1} showing an ^{18}O-shift of c. 35 cm^{-1} (^{18}O-shift = 34.2 for $HC(^{16}O)H/HC(^{18}O)H$).[27] Very weak bands situated at 1718.4, 1717.2, and 1715.8 cm^{-1} (Table 4) are assigned to $\nu_{C=O}$ and tentatively attributed to HC(O)H strongly perturbed by two hydrogen halides of the nearest neighbor in the matrix, e.g., $HC(O)H\cdots(HCl)_2$. In the $^{18}O_3$ experiment, bands attributed to $HC(^{18}O)H\cdots HCl$ were detected between 1700.0 and 1696.0 cm^{-1}. Warming experiments caused little change to the intensities of the $\nu_{C=O}$ bands; however bands attributed to $HC(^{16}O)H\cdots HBr$ intensified slightly, whereas those attributed to $HC(^{18}O)Br\cdots HBr$ and $HC(^{18}O)H$ increased markedly.

Carbon Monoxide Species. Bands appearing in the $\nu_{C\equiv O}$ region were first detected after UV−vis irradiation ($\lambda > 350$ nm) and their intensities increased dramatically upon Pyrex- ($\lambda > 290$ nm) and quartz-filtered ($\lambda > 240$ nm) irradiation. Carbon monoxide can form an array of Lewis acid complexes, giving rise to many bands in the $\nu_{C\equiv O}$ region.

OC···HX (where X = Br or Cl). After photolysis of BrCH=CHBr/O_3/Ar matrices, weak bands were detected at 2153.0 and 2150.8 cm^{-1} and assigned to $\nu_{C\equiv O}$ (Table 5 and Figure 3), while a very weak band was detected at 2504.4 cm^{-1}

TABLE 5: Infrared Bands (cm^{-1}) Assigned to $\nu_{C\equiv O}$ and Detected after Quartz-Filtered (λ > 240 nm) Irradiation of Different Matrices Containing *cis*- and *trans*-BrCH=CHBr at 14 K

$^{16}O_3$/Ar	$^{18}O_3$/Ar	$^{16}O_{3-x}{}^{18}O_x$/Ar	O_2	species
		2156.4vw, sh[a]		
		2154.5vw, sh	2154.7vw, sh	$^{16}OC\cdots(HBr)_2$[b]
		2153.9 vw, sh[a]		
2153.0w, sh[a]		2153.1vw[a]	2152.5vw, sh[a]	$^{16}OC\cdots HBr$[b]
2150.8w, sh		2151.6vw, sh	2150.4w, sh	
			2148.9w[a]	$^{16}OC\cdots H_2O$[c]
		2147.6vw, sh	2147.7w, sh	
		2146.0vw, sh	2146.8w, sh	$^{16}OC\cdots H_2O$[c]
2145.6mw, sh			2145.5w	or
			2145.0w, sh	$(C^{16}O)_x$[a]
2140.5mw[a]			2140.6w, sh[a]	$(C^{16}O)_2$
2139.3mw, sh			2139.3w	
2138.6mw, sh[a]			2138.7w, sh[a]	
2138.1mw		2138.1vw	2138.0w, sh	$C^{16}O$
			2137.2w, sh[a]	
2136.7mw, sh[a]			2136.2w[a]	
	2131.3w[a]			$^{18}OC\cdots(HBr)_2$[b]
	2128.2w			
	2106.1vw	*d*		$^{18}OC\cdots HBr$[b]
	2100.8vw[a]			
	2087.5vw	*d*		$C^{18}O$
	2086.9vw, sh[a]			

[a] Bands due to aggregates or to matrix site effects. [b] HBr of the nearest neighbor. [c] H_2O impurity. [d] Obscured by O_3 precursor bands.

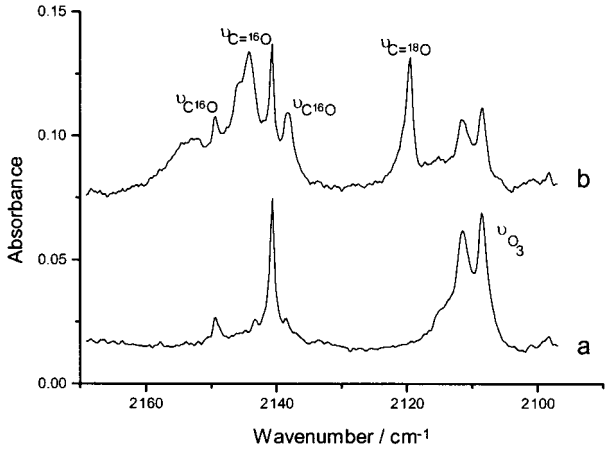

Figure 3. Infrared spectra of a BrCH=CHBr/$^{16}O_{3-x}{}^{18}O_x$/Ar matrix after (a) deposition and (b) quartz-filtered photolysis (λ > 240 nm). The spectra show the growth of new bands assigned to $\nu_{C\equiv O}$ and $\nu_{C=O}$ (BrHC=C=O).

and assigned to ν_{H-Br} (Table 6). The fact that $\nu_{C\equiv O}$ is shifted to higher wavenumber than for isolated CO (~2138 cm^{-1})[40-42] suggests that carbon monoxide is present in a perturbing environment. Similarly, the shift of ν_{H-Br} to lower wavenumber from that of isolated HBr (2568.4, 2559.6, 2549.6, and 2540.8 cm^{-1})[41,43,44] suggests that HBr is also part of the perturbing environment (Figure 4). Therefore, these bands are attributed to the carbon monoxide···Lewis acid complex OC···HBr based on the band wavenumbers reported elsewhere for OC···HBr,[34] viz. $\nu_{C\equiv O}$ = 2152 cm^{-1} and ν_{H-Br} = 2518−2502 cm^{-1}. Bands belonging to the isotopic counterpart, $^{18}OC\cdots HBr$ could be detected in the ^{18}O enriched experiments; here $\nu_{C\equiv O}$ occurred at 2106.1 and 2100.8 cm^{-1} giving an isotopic shift of ~50 cm^{-1} ($\nu_{C\equiv{}^{16}O}$ = 2138 cm^{-1}, $\nu_{C\equiv{}^{18}O}$ = 2087 cm^{-1}, ^{18}O-shift = 51 cm^{-1})[32] (Figure 3). Greater wavenumber shifts are observed for the $\nu_{C\equiv O}$ and ν_{H-Br} bands of the $OC\cdots(HBr)_2$ complex (Tables 5 and 6), and the values closely match those observed for $OC\cdots(HBr)_2$ studied elsewhere.[27,34] The bands for $^{18}OC\cdots(HBr)_2$ are listed in Tables 5 and 6. Warming of the matrix caused the intensities of some bands belonging to $OC\cdots(HBr)_2$ to decrease while new bands, probably belonging to $OC\cdots(HBr)_x$ (x > 2) appeared.

TABLE 6: Infrared Bands (cm^{-1}) Detected after Photolysis (λ > 240 nm) of *cis*- and *trans*-BrCH=CHBr in Different Matrices at 14 K

$^{16}O_3$/Ar	$^{18}O_3$/Ar	$^{16}O_{3-x}{}^{18}O_x$/Ar	assignment
2504.4vw	2505.2vw	2505.1vw	ν_{H-Br}[a] (OC···HBr)
	2499.1vw, sh[b]		or (OC···**HBr**···HBr)[c]
	2490.7vw[b]	2490.7vw[b]	
2488.3w, sh	2488.6w	2488.8vw	
2479.6w, sh[b]	2487.4vw, sh[b]	2488.0vw[b]	
2471.7w[b]		2474.8vw[b]	ν_{H-Br}[d]
2464.2w[b]		2464.4vw[b]	(OC···HBr···**HBr**)[c]
2457.1w[b]			
2446.0w, sh[b]			
2424.7w[b]			
2143.6mw		2144.1w	$\nu_{C=^{16}O}$ (BrHC=C=O)
2142.0mw, sh[b]			
	2120.4mw, sh[b]	2120.5w, sh[b]	
	2119.5m	2119.7w	$\nu_{C=^{18}O}$ (BrHC=C=O)
	2116.6w, sh[b]		
	2113.2w, sh[b]		
	1267.0w[b]		δ_{CH} (HC(O)H)
1264.1w, sh	1265.2w	1265.2w	or epoxy group **?**
1218.1vw[b]		1218.5vw[b]	
	1210.8vw[b]		
1200.3vw	1200.8vw		δ_{CHBr} (SOZ) **?**
	1199.3vw, sh[b]		
1197.8vw[b]	1198.6vw[b]	1198.7vw	
1145.4mw, sh			
1142.0mw		1142.1vw	
1140.8mw, sh			δ_{CHBr}[b] (SOZ)
1130.9w			or epoxy group **?**
	1125.4vw	1126.3vw	
	1122.2w		
	1107.0vw	1111.9vw	$\nu_{C=C}$ (BrHC=C=O)
1060.6vw		1060.5vw[e]	$\nu_{C-^{16}O}$ (SOZ) **?**
1060.0vw, sh			
	1042.7vw	*e*	$\nu_{C-^{18}O}$ (SOZ) **?**
799.6vw	801.1vw[f]	799.7vw	$\nu^{16}{}_{O-^{16}O}$ (SOZ)[g] or
	771.6vw[f]		ring bend (SOZ) **?**
	766.8vw, sh[b]		$\nu^{18}{}_{O-^{18}O}$ (SOZ)[g] or
	765.2w	765.6vw	ring bend (SOZ) **?**
	760.8, sh[b]		
637.2vw	636.9w		ν_{C-Br} (HC(O)Br) or
	631.9vw[b]		ring bend (SOZ) **?**

[a] A very weak band detected at 2502.3 cm^{-1} in the O_2 matrix is assigned to ν_{H-Br} (OC···HBr). [b] Bands due to aggregates or to matrix site effects. [c] Bold denotes the position of HBr to which the wavenumber refers. [d] A very weak band detected at 2497.7 cm^{-1} in the O_2 matrix is assigned to ν_{H-Br} ($OC\cdots(HBr)_2$). [e] Bands obscured by O_3 bands. [f] ^{16}O impurity? [g] No $^{16}O^{18}O$ isotopomer band detected.

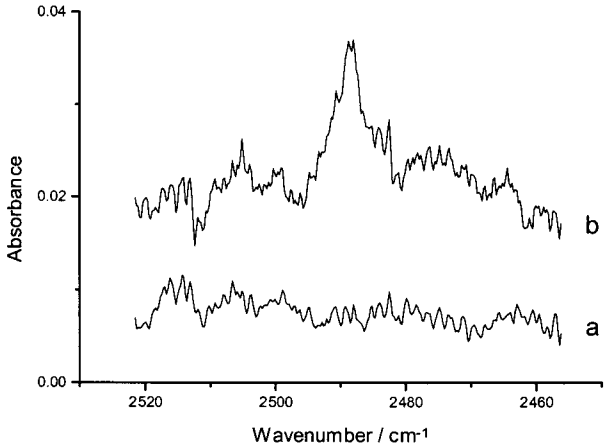

Figure 4. Infrared spectra of a BrCH=CHBr/$^{16}O_{3-x}{}^{18}O_x$/Ar matrix after (a) deposition and (b) quartz-filtered photolysis (λ > 240 nm) showing new bands assigned to ν_{H-Br} of different species.

TABLE 7: Infrared Bands (cm^{-1}) Assigned to $\nu_{C\equiv O}$ and Detected after Quartz-Filtered (λ > 240 nm) Irradiation of Matrices Containing *trans*-ClCH=CHCl at 14 K

$^{16}O_3$/Ar	$^{18}O_3$/Ar	$^{16}O_{3-x}{}^{18}O_x$/Ar	O_2	species
2160.2w[a]				$^{16}OC\cdots(HCl)_2$[b]
2157.7w		2159.3w, sh		
2155.5w, sh				$HCl\cdots C^{16}O\cdots HCl$[b]
2151.1w, sh[a]		2151.1m, sh[a]	2151.2w, sh[a]	$^{16}OC\cdots HCl$[b]
		2148.7m, sh		$^{16}OC\cdots H_2O$[c] or $(CO)_x$?
2146.9w, sh		2146.2m		
2145.7w				
2143.4w		2142.1mw, sh	2142.5mw	
2138.5vw, sh		2138.0w, sh		$C^{16}O$
	2104.8w, sh[a]			$^{18}OC\cdots(HCl)_2$[b]
	2103.5w			
	2101.9w[a]	2100.3w[a]		$^{18}OC\cdots HCl$[b]
	2097.3w	2097.3w		
	2093.6w, sh	2094.4w, sh		$^{18}OC\cdots H_2O$[c] or $(C^{18}O)_x$
	2091.9w	2093.1w, sh		
	2090.8w	2092.0w		
	2088.2w, sh[a]	2090.8w[a]		$C^{18}O$
		2087.6w, sh		
	2086.6w[a]	2086.8w[a]		

[a] Bands due to aggregates or to matrix site effects. [b] HCl of the nearest neighbor. [c] H_2O impurity.

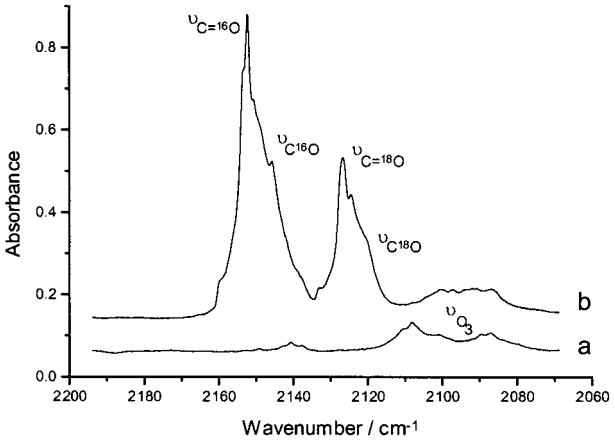

Figure 5. Infrared spectra of a ClCH=CHCl/$^{16}O_{3-x}{}^{18}O_x$/Ar matrix after (a) deposition and (b) quartz-filtered irradiation (λ > 240 nm). New bands are assigned to $\nu_{C\equiv O}$ and $\nu_{C=O}$ (ClHC=C=O) of each isotopomer.

Similarly, in the ClCH=CHCl/O_3 matrix experiment, a band detected after photolysis at 2151.1 cm^{-1} is assigned to a perturbed C≡O stretch of the complex OC···HCl (Table 7 and Figure 5). The ν_{H-Cl} bands associated with this complex occurred at 2809.4 cm^{-1} (isolated HCl in solid argon absorbs between 2888.0 and 2853.3 cm^{-1})[41,43,45] (Table 8 and Figure 6). For comparison, $\nu_{C\equiv O}$ bands occurred at 2154.2 and 2152.2 cm^{-1} and ν_{H-Cl} bands occurred at 2815.3 and 2810.2 cm^{-1} for OC···HCl studied elsewhere.[41,35] Bands belonging to the ^{18}OC···HCl isotopomer were detected around 2097.3 cm^{-1} (Table 7). Some $\nu_{C\equiv O}$ bands experienced large wavenumber shifts to 2160.2 and 2157.7 cm^{-1} from that of isolated CO (~2138 cm^{-1});[40-42] they are thus attributed to OC···$(HCl)_2$ based on the fact that $\nu_{C\equiv O}$ bands of similar wavenumber were obtained for this complex elsewhere.[27,41] The ν_{H-Cl} bands of OC···$(HCl)_2$ appeared around 2788.0 cm^{-1} in the mixed-ozone experiment (ν_{H-Cl} = 2788.2 cm^{-1} for OC···$(HCl)_2$).[43] The $\nu_{C\equiv O}$ bands for the ^{18}OC···$(HCl)_2$ isotopomer (Table 7) are at similar wavenumbers to those detected elsewhere for this species.[27] A weak shoulder situated at 2155.5 cm^{-1} and a weak band at 2800.5 cm^{-1} are assigned to $\nu_{C\equiv O}$ and ν_{H-Cl}, respectively, of HCl···OC···HCl as these wavenumbers are intermediate between those of OC···$(HCl)_2$ and OC···HCl. No significant changes to the $\nu_{C\equiv O}$ bands were observed in warming experiments, except in the $^{18}O_3$ experiment, during which the intensities of bands attributed to OC···$(HCl)_2$ decreased. A slight decrease in the intensities of ν_{H-Cl} bands belonging to OC···$(HCl)_2$ was also observed.

TABLE 8: Infrared Bands (cm^{-1}) Detected after Quartz-Filtered (λ > 240 nm) Photolysis of Different Matrices Containing *trans*-ClCH=CHCl at 14 K

$^{16}O_3$/Ar	$^{18}O_3$/Ar	$^{16}O_{3-x}{}^{18}O_x$/Ar	assignment
a	2826.9w	2826.2vw	ν_{H-Cl}[c] $(HCl)_2$
	2819.5w[b]		
a	2809.4w	2809.4w	ν_{H-Cl}[d] (OC···HCl) or (OC···HCl···**HCl**)
a	2800.5w	2800.0w	ν_{H-Cl} (HCl···CO···HCl)
		2791.8w, sh[b]	ν_{H-Cl}[e] (OC···**HCl**···HCl)
a	2788.2w	2788.0w, sh	
		2784.8w, sh[b]	
	2764.2vw[b]		
	2753.7vw[b]		
	2735.8vw[b]		
	2261.6vw	2261.6vw	$\nu_{C\equiv C}$[b,f]
		2247.4vw	
	2242.8vw	2242.5vw	
2230.8vw		2231.0vw	
2227.7vw	2223.9vw	2224.4vw	
2223.9vw, sh	2220.7w		
2153.6w[b]		2153.6m, sh[b]	$\nu_{C=^{16}O}$ (ClHC=C=O)
2152.4w		2152.3ms	
	2133.2mw[b]	2132.9w, sh[b]	$\nu_{C=^{18}O}$ (ClHC=C=O)
	2130.5mw, sh[b]		
	2126.8ms	2127.0m	
	2124.7m[b]	2124.2mw, sh[b]	
	2121.3mw, sh[b]	2120.9mw, sh[b]	
	1288.7vw		δ_{HCH}[b] (HC(O)H) or epoxy group ?
1280.0vw	1287.0vw, sh		
1272.0vw	1276.9vw		
	1269.7vw	1269.5w	
	1265.3vw, sh		
1244.2vw	1240.7vw, sh	1244.1w	
	1237.2vw		
1218.3vw	1218.1vw	1218.3vw	δ_{CHCl} (SOZ) ?
		1168.9vw	δ_{CHCl}[b] (SOZ) or epoxy group ?
a		1166.3vw	
	1148.5w	1148.3vw	
		1134.5vw	
	1110.9vw		$\nu_{C=C}$ (ClHC=C=O)[b]
a	1106.1vw	1108.1vw	
	1098.4vw	1099.9vw	
1083.7vw		1083.6w	$\nu_{C-^{16}O}$ (SOZ) ?
		1079.7w, sh[b]	
	1067.7mw	1067.6w	$\nu_{C-^{18}O}$ (SOZ) ?
	1064.7w, sh[b]	1064.6vw, sh[b]	
1053.2vw	1052.4w	1052.9vw	δ_{OCO} (SOZ) ?
a		889.3vw[b]	$\nu_{C-^{18}O}$ (SOZ) or epoxy group ?
	885.5vw	885.5vw	
a	796.4w[g]	796.4vw	$\nu^{16}{}_{O-^{16}O}$ (SOZ)[h] or ring bend (SOZ) ?
	784.5w[g]		
	762.5w, sh	764.9w, sh	$\nu^{18}{}_{O-^{18}O}$ (SOZ)[h] ?
758.7vw	756.8mw	757.0mw, sh	ν_{C-Cl}[b] (SOZ) ?
748.6vw	745.2mw, sh	748.4mw	
731.0vw	731.0mw	731.0mw	ring bend[b] (SOZ) or ν_{C-Cl}[i] (HC(O)Cl) ?
		729.0mw	
728.7vw	728.7mw	723.5w, sh	
	716.8w	716.8w	
		657.3mw	ring bend (SOZ) ?
a	652.3mw	652.6mw, sh[b]	
	648.0mw[b]		

[a] Bands too weak to be detected. [b] Bands due to aggregates or to matrix site effects. [c] A very weak band detected at 2822.0 cm^{-1} in the O_2 matrix is assigned to ν_{H-Cl} $(HCl)_2$. [d] A very weak band detected at 2808.2 cm^{-1} in the O_2 matrix is assigned to ν_{H-Cl} (OC···HCl). [e] Very weak bands detected at 2793.0, 2791.5, and 2787.2 cm^{-1} in the O_2 matrix are assigned to ν_{H-Cl} (OC···**HCl**···HCl). [f] Matrix environment or complex formation makes $\nu_{C\equiv C}$ IR active. [g] ^{16}O impurity? [h] No $^{16}O^{18}O$ isotopomer detected. [i] Bands due to isotopic splitting or to site effects.

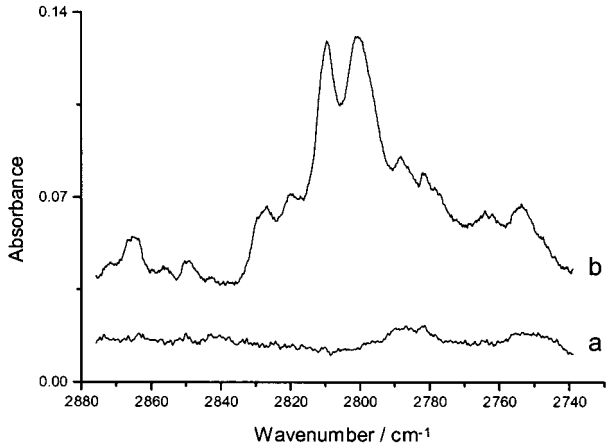

Figure 6. Infrared spectra of a ClCH═CHCl/$^{18}O_3$/Ar matrix after (a) deposition and (b) quartz-filtered photolysis (λ > 240 nm) showing bands appearing in the ν_{H-Cl} region.

These observations can be rationalized as follows: The 5σ orbital of CO has been shown to be weakly antibonding and, being located on the C atom, the removal of electron density therefrom to the Lewis acid HCl or HBr results in an increase both in the CO bond strength and in $\nu_{C\equiv O}$.[41,46] Complete ionization raises $\nu_{C\equiv O}$ from 2143 cm^{-1} ($CO_{(g)}$) to 2184 cm^{-1} ($CO^+_{(g)}$).[41,47] The transfer of electron density from the 5σ orbital of CO to the σ* HX orbital (antibonding) causes the H−X bond to weaken and thus ν_{H-X} to drop in wavenumber from its value for isolated HX.

Ketene. Bands attributable to a ketene type species BrHC═C═O, were first detected after UV−vis irradiation of BrCH═CHBr/O_3 matrices, and their intensities continued to increase after Pyrex- and quartz-filtered irradiation (Table 6 and Figure 3). The medium weak bands at 2143.6 and 2142.0 cm^{-1} are assigned to $\nu_{C=O}$ of BrHC═C═O, whereas bands detected for the ^{18}O counterpart occurred between 2120.4 and 2113.2 cm^{-1} and are assigned to $\nu_{C=O}$ of the isotopomer BrHC═C═^{18}O. Both sets of bands were detected in the mixed-ozone experiment highlighting the contribution from one O atom to the vibrational mode $\nu_{C=O}$. The C═C stretch of BrHC═C═O occurred at 1107.0 and 1111.9 cm^{-1} in the $^{18}O_3$ and $^{16}O_{3-x}{}^{18}O_x$ experiments, respectively. For comparison, the $\nu_{C=O}$ and $\nu_{C=C}$ bands detected elsewhere for the ketene species H_2C═C═O appeared at 2142.2 cm^{-1} (^{18}O at 2115.4 cm^{-1})[48,49] and 1111.4 cm^{-1} (^{18}O at 1108.0 cm^{-1}),[48,49] respectively. The bands arising from other vibrational modes of BrHC═C═O were either too weak to be detected or were hidden by precursor or product bands. The UV−vis photolysis of ClCH═CHCl/O_3/Ar matrices also resulted in the appearance of new bands which are attributed to the ketene species ClHC═C═O (Table 8 and Figure 5). The intensities of these bands increased after Pyrex- and quartz-filtered irradiation. Those at 2153.6 and 2152.4 cm^{-1} are assigned to $\nu_{C=O}$, whereas the ^{18}O counterpart bands occurred around 2126.8 cm^{-1} (bands belonging to both isotopomers were found in the mixed-ozone experiment). Bands attributable to the C═C stretch of ClHC═C═O were detected in the $^{18}O_3$ and $^{16}O_{3-x}{}^{18}O_x$ experiments between 1110.9 and 1098.4 cm^{-1} and at 1108.1 and 1099.9 cm^{-1}, respectively. The $\nu_{C=O}$ and $\nu_{C=C}$ band wavenumbers detected here are similar to those observed for H_2C═C═O as studied elsewhere.[48,49]

Other Species. A number of new bands appeared after prolonged photolysis cycles (24 h) using quartz-filtered (λ > 240 nm) radiation of both BrCH═CHBr/O_3/Ar and ClCH═CHCl/O_3/Ar matrices. The bands suggest the possible presence of a secondary ozonide (SOZ) in each case (Tables 6 and 8) because bands at similar wavenumbers were obtained for 1,2,4-trioxolane (SOZ) detected in experiments on CH_2═CH_2/O_3.[2,20] However, the identification of SOZ species remains uncertain owing to the weakness and incompleteness of the bands detected and possibly attributable to this species and to the very low probability of large fragments (carbonyl oxide and HC(O)X) recombining to form a new five-membered ring in a rigid matrix environment. A further study using quantum chemical methods could provide the information needed to determine whether the SOZ species is actually present in the matrix.

Some of the bands already discussed could belong to other species. For example, ethene oxide has been studied by a number of groups[28,37,50] who have associated bands at 1265, 1165, and 865 cm^{-1} with the epoxy group. Bands detected at 1264.1 and near 1145.4 cm^{-1} (Table 6), attributed to a HC(O)H and a possible SOZ species, respectively, could also be attributed to an epoxy group of a species formed after photolysis of BrCH═CHBr/O_3/Ar matrices, although no bands appeared close to 865 cm^{-1}. Likewise, the photoinduced reaction between ClCH═CHCl and O_3 formed bands near 1272, 1148, and 885 cm^{-1} (Table 8) which could also be attributed to an epoxide species. In other studies of halogenoethene reactions,[19,20] it was proposed that cyclopropane could form, but the characteristic ring bending mode giving rise to a band near 1020−1000 cm^{-1} [28] could not be detected in the present experiments. Carboxylic acids have also been detected among the many reaction products of alkene/O_3 reactions, but there is no evidence here to suggest that any carboxylic acids or other O−H species were formed in these experiments as no ν_{O-H} bands were detected.

In the ClCH═CHCl/O_3 matrix experiments, many bands occurred in the C≡C stretching region (Table 8) and are thus assigned to $\nu_{C\equiv C}$, probably of C_2Cl_2 as no ≡C−H bands were detected and $\nu_{C\equiv C}$ of disubstituted alkynes occurs in the region of 2260−2190 cm^{-1}.[28] Either the matrix environment or the existence of a C_2Cl_2···Lewis acid complex must have removed the symmetry of C_2Cl_2 for $\nu_{C\equiv C}$ to become infrared active.

Solid Oxygen Matrices. Prolonged quartz-filtered (λ > 240 nm) irradiation of BrCH═CHBr or ClCH═CHCl deposited in solid oxygen matrices produced similar bands to those produced in the BrCH═CHBr/O_3 or ClCH═CHCl/O_3 experiments, respectively, and are assigned on this basis (Tables 3, 4, 5, and 7). No complex is formed and so long photolysis periods were required to initiate the reaction. The oxygen matrix acts as an oxygen atom source to produce the oxygenated products, C═O, C≡O, and BrHC═C═O/ClHC═C═O species. These oxygen matrix experiments therefore highlight the fact that the carbonyl and carbon monoxide species are produced via a pathway alternative to ozonolysis via the Criegee mechanism. Warming experiments led to an increase in intensity of the $\nu_{C\equiv O}$ bands between 2154.7 and 2145.0 cm^{-1} at the expense of those between 2140.6 and 2136.2 cm^{-1} indicating a preference toward the formation of carbon monoxide complexes (Table 5).

Photochemical Pathway. The first step in the photochemical pathway (Scheme 1) is the formation of a charge-transfer complex between ozone and the π system of BrCH═CHBr or ClCH═CHCl after co-deposition of each precursor in solid argon. The detection of other charge-transfer complexes between ozone and sp^2 systems has been reported in several studies.[8,15−18] The complex could be of a σ-type which favors the formation of an epoxide via O_2 loss, although bands tentatively attributed to an epoxide appeared only after prolonged UV irradiation, suggesting first the dissociation of ozone followed by the addition of an O(^{1}D) atom to form the epoxide (Scheme 2, (iii)). The π charge-transfer complex allows ozone to photodissociate

SCHEME 1

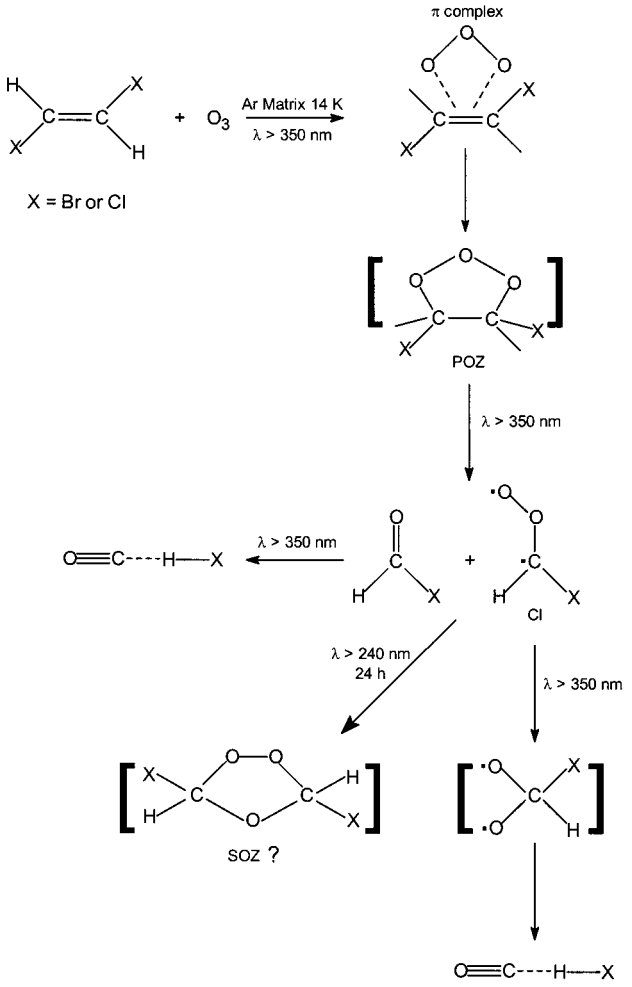

at wavelengths longer than those required to dissociate isolated ozone (UV irradiation into the Hartley band at 200−310 nm forms excited-state atomic oxygen, $O(^1D)$, and molecular oxygen). Hence, photolysis with radiation of wavelengths > 350 nm caused new bands to form in the FT-IR spectrum at the expense of bands of the complex; the new bands are attributed to $\nu_{C=O}$ and $\nu_{C\equiv O}$ of different carbonyl···Lewis acid and carbon monoxide···Lewis acid complexes, respectively. By contrast, the lack of ozone complexation in the halogenated alkane/ozone reactions[26,27] meant that quartz-filtered irradiation (λ > 240 nm) for tens of hours was necessary before new $\nu_{C=O}$ and $\nu_{C\equiv O}$ bands could form.

The carbonyl compounds have also been formed in the analogous gas and liquid-phase alkene/ozone reactions as intermediates in the ozonolysis reaction via the Criegee mechanism. Thus, the haloalkene/ozone reactions here are believed to follow the same pathway, in which the π complex undergoes a 1,3-dipolar cycloaddition to form the five-membered ring of the POZ. The POZ then cleaves to form the carbonyl oxide (Criegee intermediate, CI, Scheme 1) and subsequently the aldehyde, HC(O)Br or HC(O)Cl. The rearrangement of 1,2- to 1,1-dihaloethene, followed by ozonolysis, could have taken place because bands attributed to HC(O)H were detected. However this rearrangement would have to occur upon deposition, i.e. without photolysis, which seems very unlikely. No bands belonging to the POZ or carbonyl oxide[51] could be detected, indicating that these must be transient species which immediately dissociate. A study of the low-temperature ozonolysis of CH_2CCl_2[20] also showed no formation of the POZ even though

SCHEME 2

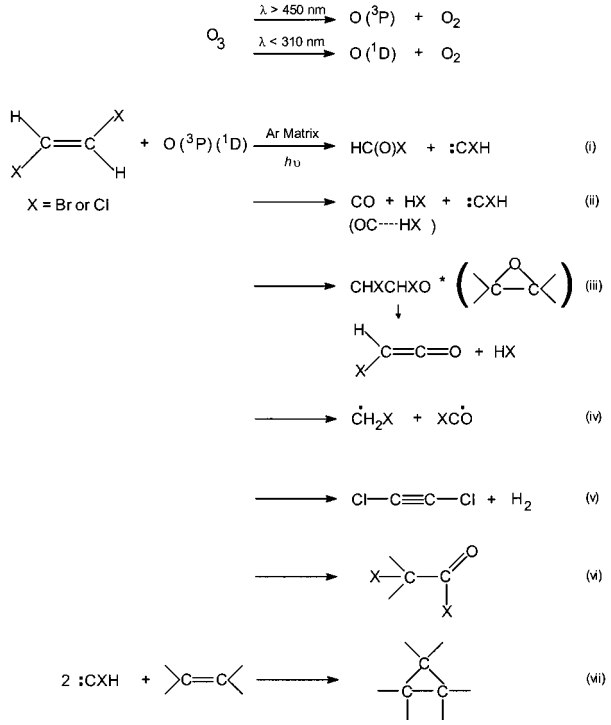

some reactions had taken place as made evident by the appearance of infrared bands of ClC(O)Cl. As reported previously[26,27,44] carbonyl complexes photodissociate to form carbon monoxide complexes, likewise HC(O)Br and HC(O)Cl detected in these experiments photodissociate to form the carbon monoxide complexes OC···HBr and OC···HCl, respectively. The formation of HC(O)X and its subsequent dissociation to form OC···HX both take place after irradiation at λ > 350 nm. The relative intensities of bands belonging to HC(O)X remained approximately constant upon photolysis at shorter wavelengths, whereas the relative intensities of bands belonging to OC···HX increased dramatically under the same photolytic conditions, indicating that a much higher percentage of the newly formed HC(O)X dissociates upon UV photolysis. This greater concentration of carbon monoxide species could also result from the simultaneous dissociation of the carbonyl oxide intermediate resulting in the elimination of CO_2, CO and HX.[7,11] Prolonged quartz-filtered photolysis produced bands that resembled those of a SOZ. Following the Criegee mechanism, the SOZ forms from the recombination of the undissociated carbonyl oxide and aldehyde HC(O)X (Scheme 1). However, the lack of conclusive evidence confirming the presence of a SOZ and the unlikely event of recombination of large fragments in a matrix environment makes the presence of a SOZ very doubtful.

The carbonyl and carbon monoxide species detected in the ozone experiments were also detected in experiments involving a solid oxygen matrix or nitrogen dioxide; this, and the fact that XHC═C═O were detected, implies that a different pathway from that of ozonolysis is being followed, one which involves the reaction of O atoms with the halogenated ethene to form similar carbonyl and carbon monoxide species. However, there are many feasible routes by which the reaction could proceed[20,21,52−54] (Scheme 2, (i)−(vii)) giving rise to intermediates that can react further; thus, the exact pathway responsible for the observed photoproducts is difficult to elucidate. The carbonyls, HC(O)Br and HC(O)Cl, and the carbon monoxide species, OC···HBr and OC···HCl, said to have been formed from the ozonolysis reaction via the Criegee mechanism, could

also occur from reaction pathways (i) and (ii), respectively (Scheme 2). The excited species CHXCHXO* represents several possible excited-state structures, including that of the epoxide (iii) which has been tentatively identified in these experiments and elsewhere.[53] The detection of bands attributable to a ketene species suggests that XHC═C═O is produced, probably by the 1,1-elimination of HX from CHXCHXO* (iii). Bands attributed to formaldehyde HC(O)H were detected but it is unclear how this species could form from XCH═CHX, unless it is via rearrangements and recombination of fragments such as those specified in pathway (iv). For HC(O)H to form via ozonolysis the 1,2-dihaloethene would first have to isomerize to form the 1,1-dihaloethene without any photolysis, or alternatively the 1,1-dihaloethene could be present as an impurity. The fairly intense $\nu_{C=O}$ bands detected for HC(O)H make these explanations doubtful. Another possibility is that photolysis of complexed XCH═CHX in the matrix could result in the elimination of H_2 or X_2 to form the alkynes XC≡CX or HC≡CH, respectively, allowing H_2 to combine with CO to form HC(O)H.[24,25] Some $\nu_{C\equiv C}$ bands were in fact detected in the ClCH═CHCl/O_3 experiment and were attributed to ClC≡CCl only, as no ν_{C-H} bands were detected (v). Because of symmetry constraints on the molecule, the $\nu_{C\equiv C}$ mode should be IR inactive; however a matrix environment of lowered symmetry or the formation of a complex of ClC≡CCl could lead to this mode being IR active. Some of the $\nu_{C=O}$ bands could also belong to an acyl halide, $CH_2XC(O)X$, formed from reaction pathway (vi). Surely, more than one species is responsible for the large number of $\nu_{C=O}$ bands detected. The diradical species formed in reaction (i) and (ii) could react with each other to form an alkane or add to XCH═CHX to form a cyclopropane (vii), although no bands indicative of these species were detected.

The photochemical reaction of either BrCH═CHBr or ClCH═CHCl with O_3 is not simple as either O_3 or O atoms or both could participate in the photochemically induced reactions via different mechanisms. It is very probable that both pathways are followed in these experiments as each produces one or other of the observed photoproducts.

Acknowledgment. The authors thank the EPSRC for financial support.

References and Notes

(1) Hull, L. A.; Hisatsune, I. C.; Heicklen, J. *J. Am. Chem. Soc.* **1972**, *94*, 4856−4864.
(2) Kuhne, H.; Gunthard, H. H. *J. Phys. Chem.* **1976**, *80*, 1238−1246.
(3) Nelander, B.; Nord, L. *Tetrahedron Lett.* **1977**, *32*, 2821−2822.
(4) Bailey, P. S. *Ozonation in Organic Chemistry*; Academic Press: New York, New York, 1978; Vol I.
(5) Harding, L. B.; Goddard, W. A. *J. Am. Chem. Soc.* **1978**, *100*, 7180−7188.
(6) Kohlmiller, C. K.; Andrews, L. *J. Am. Chem. Soc.* **1981**, *103*, 2578−2583.
(7) Atkinson, R.; Carter, W. P. L. *Chem. Rev.* **1984**, *84*, 437−470.
(8) McKee, M. L.; McMichael, R. C. *J. Am. Chem. Soc*. **1989**, *111*, 2497−2500.
(9) Samuni, U.; Fraenkel, R.; Haas, Y.; Fajgar, R.; Pola, J. *J. Am. Chem. Soc.* **1996**, *118*, 3687−3693.
(10) Horie, O.; Schafer, C.; Moortgat, G. K. *Int. J. Chem. Kinet.* **1999**, *31*, 261−269.
(11) Anglada, J. A.; Crehuet, R.; Bofill, J. M. *Chem. Eur. J.* **1999**, *5*, 1809−1822.
(12) Neeb, P.; Moortgat, G. K. *J. Phys. Chem.* **1999**, *103*, 9003−9012.
(13) Atkinson, R. *Atmos. Environ.* **1990**, *24A*, 1−41.
(14) Criegee, R. *Angew. Chem., Int. Ed. Engl.* **1975**, *14*, 745−752.
(15) Bailey, P. S.; Ward, J. W.; Hornish, R. E. *J. Am. Chem. Soc.* **1971**, *93*, 3552−3554.
(16) Bailey, P. S.; Ward, J. W.; Carter, T. P.; Neih, E.; Fischer, C. M.; Khashab, A. Y. *J. Am. Chem. Soc.* **1974**, *96*, 6136−6140.
(17) Jonnalagadda, S.; Chan, S.; Garrido, J.; Bond, J.; Singmaster, K. A. *J. Am. Chem. Soc.* **1995**, *117*, 562−563.
(18) Singmaster, K. A.; Pimentel, G. C. *J. Phys. Chem.* **1990**, *94*, 5226−5229.
(19) Sanhueza, E.; Heicklen, J. *Int. J. Chem. Kinet.* **1975**, *7*, 589−604.
(20) Sanhueza, E.; Hisatsune, I. C.; Heicklen, J. *Chem. Rev.* **1976**, *76*, 801−826.
(21) Griesbaum, K.; Hayes, M. P.; Werli, V. *Can. J. Chem.* **1988**, *66*, 1366−1370.
(22) Hasson, A. S.; Smith, I. W. M. *J. Phys. Chem. A* **1999**, *103*, 2031−2043.
(23) Cartland, H. E.; Pimentel, G. C. *J. Phys. Chem.* **1986**, *90*, 5485−5491.
(24) Laursen, S. L.; Pimentel, G. C. *J. Phys. Chem.* **1989**, *93*, 2328−2333.
(25) Laursen, S. L.; Pimentel, G. C. *J. Phys. Chem.* **1990**, *94*, 8175−8182.
(26) Clark, R. J. H.; Dann, J. R. *J. Phys. Chem. A* **1997**, *101*, 2074−2082.
(27) Lugez, C.; Schriver, A.; Schriver-Mazzuoli, L.; Lasson, E.; Nielsen, C. J. *J. Phys. Chem.* **1993**, *97*, 11 617−11 624.
(28) Bellamy, L. J. *The Infrared Spectra of Complex Molecules;* Wiley: New York, 1975.
(29) Cowieson, D. R.; Barnes, A. J.; Orville-Thomas, W. J. *J. Raman Spectrosc.* **1981**, *10*, 224−226.
(30) Rytter, E.; Gruen, D. M. *Spectrochim. Acta* **1979**, *35A*, 199−207.
(31) Brosset, P.; Dahoo, R.; Gauthier-Roy, B.; Abouaf-Marguin, L.; Lakhlifi, A. *Chem. Phys.* **1993**, *172*, 315−324.
(32) Schriver-Mazzuoli, L.; de Saxce, A.; Lugez, C.; Camy-Peyret, C.; Schriver, A. *J. Chem. Phys.* **1995**, *102*, 690−701.
(33) Dimitrov, A.; Seppelt, K.; Scheffler, D.; Willner, H. *J. Am. Chem. Soc.* **1998**, *120*, 8711−8714.
(34) Lasson, E.; Nielsen, C. J. *Acta Chem. Scand.* **1997**, *51*, 1−7.
(35) Strandman-Long, L.; Nelander, B.; Nord, L. *J. Mol. Struct.* **1984**, *117*, 217−233.
(36) Khoshkhoo, H.; Nixon, E. R. *Spectrochim. Acta* **1973**, *29A*, 603−612.
(37) Herzberg, G. *Infrared and Raman Spectra of Polyatomic Molecules*; Van Nostrand: New York, 1945.
(38) Nelander, B. *J. Chem. Phys.* **1980**, *73*, 1026−1033.
(39) Nelander, B. *J. Mol. Struct.* **1980**, *69*, 59−68.
(40) Dubost, H.; Abouaf-Marguin, L. *Chem. Phys. Lett.* **1972**, *17*, 269−273.
(41) Andrews, L.; Arlinghaus, R. T.; Johnson, G. L. *J. Chem. Phys.* **1983**, *78*, 6347−6352.
(42) Loewenschuss, A.; Givan, A.; Nielsen, C. J. *J. Mol. Struct.* **1997**, *408/409*, 533−537.
(43) Barnes, A. J.; Hallam, H. E.; Scrimshaw, G. F. *Trans. Faraday Soc.* **1969**, *65*, 3172−3178.
(44) Clark, R. J. H.; Dann, J. R.; Foley, L. J. *J. Chem. Soc., Dalton Trans.* **1999**, 73−78.
(45) Barnes, A. J.; Hallam, H. E.; Scrimshaw, G. F. *Trans. Faraday Soc.* **1969**, *65*, 3150−3158.
(46) Huo, W. M. *J. Chem. Phys.* **1965**, *43*, 624−628.
(47) Rosen, B. *Spectroscopic Data Relative to Diatomic Molecules*; Pergamon: New York, 1970.
(48) Hochstrasser, R.; Wirz, J. *Angew. Chem., Int. Ed. Engl.* **1990**, *29*, 411−413.
(49) Moore, C. B.; Pimentel, G. C. *J. Chem. Phys.* **1963**, *38*, 2816−2829.
(50) Lord, R. C.; Nolin, B. *J. Chem. Phys.* **1956**, *24*, 656−658.
(51) Sander, W. *Angew. Chem., Int. Ed. Engl.* **1990**, *29*, 344−354.
(52) Fitzmaurice, D. J.; Frei, H. *J. Phys. Chem.* **1992**, *96*, 10308−10315.
(53) Bosch, E.; Kochi, J. K. *J. Am. Chem. Soc*. **1996**, *118*, 1319−1329.
(54) Chatterjee, J.; Coombes, R. G.; Barnes, J. R.; Fildes, M. J. *J. Chem. Soc., Perkin Trans. 2* **1995**, 1031−1032.